



# Optical properties, morphology and elemental composition of atmospheric particles at T1 supersite on MILAGRO campaign

G. Carabali<sup>1</sup>, R. Mamani-Paco<sup>1</sup>, T. Castro<sup>1</sup>, O. Peralta<sup>1</sup>, E. Herrera<sup>2</sup>, and B. Trujillo<sup>2</sup>

<sup>1</sup>Centro de Ciencias de la Atmósfera, UNAM, Ciudad de México, DF, México

<sup>2</sup>Centro de Investigaciones de Materiales Avanzados, Chihuahua, México

Correspondence to: T. Castro (telma@atmosfera.unam.mx)

Received: 4 April 2011 – Published in Atmos. Chem. Phys. Discuss.: 25 May 2011

Revised: 30 January 2012 – Accepted: 17 February 2012 – Published: 14 March 2012

**Abstract.** Atmospheric particles were sampled at T1 supersite during MILAGRO campaign, in March 2006. T1 was located at the north of Mexico City (MC). Aerosol sampling was done by placing copper grids for Transmission Electron Microscope (TEM) on the last five of an 8-stage MOUDI cascade impactor. Samples were obtained at different periods to observe possible variations on morphology. Absorption and scattering coefficients, as well as particle concentrations (0.01–3  $\mu\text{m}$  aerodynamic diameter) were measured simultaneously using a PSAP absorption photometer, a portable integrating nephelometer, and a CPC particle counter. Particle images were acquired at different magnifications using a CM 200 Phillips TEM-EDAX system, and then calculated the border-based fractal dimension. Also, Energy Dispersive X-Ray Spectroscopy (EDS) was used to determine the elemental composition of particles. The morphology of atmospheric particles for two aerodynamic diameters (0.18 and 1.8  $\mu\text{m}$ ) was compared using border-based fractal dimension to relate it to the other particle properties, because T1-generated particles have optical, morphological and chemical properties different from those transported by the MC plume.

Particles sampled under MC pollution influence showed not much variability, suggesting that more spherical particles (border-based fractal dimension close to 1.0) are more common in larger sizes ( $d_{50} = 1.8 \mu\text{m}$ ), which may be attributed to aerosol aging and secondary aerosol formation. Between 06:00 and 09:00 a.m., smaller particles ( $d_{50} = 0.18 \mu\text{m}$ ) had more irregular shapes resulting in higher border-based fractal dimensions (1.2–1.3) for samples with more local influence. EDS analysis in  $d_{50} = 0.18 \mu\text{m}$  particles showed high contents of carbonaceous material, Si, Fe, K, and Co. Perhaps, this indicates an impact from industrial and vehicle emissions on atmospheric particles at T1.

## 1 Introduction

Most megacities in the developing world lie in subtropical and tropical latitudes, with a population growth so intensive that urban areas are constantly increasing without adequate planning. Mexico City (MC) is one of those, it is located at 2240 m above sea level, and has high solar irradiance, light winds and heterogeneous atmospheric removal processes (Raga et al., 2001) that are quite different from other megacities at mid-latitudes. This situation is moreover complicated by the plumes from the Popocatepetl volcano, a natural source of gases and sulfate enriched aerosols. During volcanic activity the plumes contain significant quantities of aerosols composed by sulfates, especially in the smaller sizes (Jiménez et al., 2004).

Light absorbing particles generated by megacities can modify climate, because they warm the atmosphere counteracting to cooling caused by particles such as sulfates that predominantly scatter light (Bond and Bergstrom, 2005). Improved understanding of particle morphology is also an important factor in modeling the effect of fine particles on the absorption and scattering of radiation in the atmosphere, which is needed for an accurate determination of the radiative forcing associated with fine atmospheric particles (Mishchenko et al., 1995) in calculating an energy balance to assess global climate change (Mamani-Paco and Helble, 2007).

Also, fine particles could directly affect human health, for instance lung and even heart diseases (Pope and Dockery, 2006). Dockery et al. (1993) showed that mortality rates were more strongly associated with levels of fine sulfate inhalable particles than with levels of aerosol acidity, total particle concentrations, sulfur dioxide or nitrogen dioxide,

respectively in six US cities. Tsuji et al. (2006) have indicated that the surface area and particle number are important in risk assessment of inhalation dosimetry of particles. Non-spherical particles have higher surface area than spherical particles of comparable aerodynamic diameter, thereby providing potentially more surface contact for lung-particle interaction.

T1 is located approximately 30 km away from MC and it has different aerosol sources based on its own local activities apart from the megacity. So, particles have physical and chemical properties that can be linked to their source or to the place where they were sampled. We tried to distinguish optical, morphological and chemical particles characteristics generated at T1, from those transported by the MC plume to the site. According to Doran et al. (2007), De Foy (2008) and Fast et al. (2007) there is a net transport of pollutants from MC to T1 and T2.

In MC, the light absorbed by atmospheric aerosols is mainly due to particles from motor vehicles exhausts, especially diesel engines (Molina and Molina, 2002). Fresh soot particles contribute most of the absorption in the early morning periods when traffic levels peak. Aged soot particles become the major absorbers when the photochemistry for nitric acid and organic compounds condense onto the soot particles surface (Salcedo et al., 2006; Paredes-Miranda et al., 2009) and contribute to decrease the particles single scattering albedo. Furthermore, soot particles in MC include nitrates and sulfates, consequential of the mixing with sulfate produced by oxidation of sulfur in the fuel followed by rapid condensation onto existing particles in the plume formed during the combustion process (Moffet and Prather, 2009). As particles age, inorganic (e.g. nitrates and sulfates) and organic species coat them (Adachi and Buseck, 2008; Moffet et al., 2010). In addition, it seems that water influences the amount of sulfates present in particles, so in days with high relative humidity a larger fraction of sulfates has been reported (Baumgardner et al., 2000).

Soot is characterized as any light absorbing combustion generated aerosol. Soot is considered as an aggregate of tiny spherules (Bond et al., 2005). As an aggregate, it collapses and becomes more like a sphere, and the light absorption decreases.

Many studies on morphology and chemical composition observed by electron microscopy (Dye et al., 2000; Xiong and Friedlander, 2001; Katrinak et al., 1993; Okada and Heintzenberg, 2003) report different shapes of atmospheric particles (spheres, aggregates, and irregular shapes), because the morphology is influenced by physical and chemical processes related to ambient conditions. Some studies classify particles using their basic elemental composition and morphology. For instance, Mogo et al. (2005), Li and Shao (2009), and Johnson et al. (2005) classify atmospheric particles into the following groups: mineral, Ca-S, S-rich, K-rich, organic, soot, fly ash, and metal.

To date, the border-based fractal dimension has been calculated for a limited number of particles, not enough to associate structural properties with temperature, relative humidity, time of the day or traffic conditions (Kidratenko et al., 1994). This study reports information about optical properties and morphology associated to border-based fractal dimension.

This research used a MOUDI impactor to sample atmospheric particles at T1 supersite during MILAGRO campaign on March 2006 (Molina et al., 2010). The morphology of individual particles was analyzed using digital images from a Transmission Electron Microscope (TEM) and then the border-based fractal dimension ( $D_f$ ) was calculated with a FORTRAN code (Newman, 2001). In addition, an Energy Dispersive X-Ray Spectroscopy (EDS) was used to get information about the elemental chemical composition for some particles. Two sampling days were compared, one of them with not a clear influence (15 March 2006) from the pollution plume produced by Mexico City, and the other one directly influenced by city emissions (19 March 2006). MOUDI cut-off sizes analyzed were  $d_{50} = 1.8$  and  $d_{50} = 0.18$   $\mu\text{m}$ .

## 2 Experimental method

### 2.1 Aerosol particles sampling

T1 was located at the Universidad Tecnológica de Tecámac, State of Mexico, with coordinates 19°43' N latitude and 98°58' W longitude; which is located at 2340 m above sea level. The site was towards the north of MC, and represented a place where emissions are fresh and well mixed (Molina et al., 2010).

To measure particle optical properties, from 1 to 31 March 2006, we placed a Particle Soot/Absorption Photometer (PSAP), which is a filter based measurement technique. The particle laden air stream first passes through a primary filter and the aerosol absorption is determined by measuring light attenuation at 550 nm. The clean air stream then passes through a second filter adjacent to the primary filter, which is used as a reference in order to ensure that the observed change in primary filter transmittance is not due to changes in the intensity of the light source. A nephelometer model M903 was used to measure scattering (Radiance Research Model 903) operating at 530 nm, calibrated by comparison to a second M903 nephelometer. Both instruments were connected to a particle counter (CPC) model 3010 (TSI, Inc.), which measures particles concentrations within 0.01–3  $\mu\text{m}$  diameter range. The sampling system was 4 m above the ground level. Data acquisition was done with one minute resolution.

Additionally, we used two eight-stage Micro Orifice Uniform Deposit Impactors (MOUDI), model MSP 100, to collect atmospheric particles every two days during the field campaign. Grids coated with collodion for the Transmission

Electron Microscope (LF-200-Cu mesh, thickness  $\sim 60$  nm) were placed on the last five stages of the MOUDI ( $d_{50} = 1.8, 1.0, 0.56, 0.32,$  and  $0.18 \mu\text{m}$ ). The MOUDI inlet flow was calibrated with a Gilibrator Air Flow Calibration System and set to 30 lpm.

To relate particle morphology to vehicular traffic emissions and atmospheric transport, we established a particle sampling schedule for 06:00–09:00, 11:00–14:00, 16:00–19:00, and 21:00–24:00, local time. We used the meso-meteorological model MM5 predictions (de Foy et al., 2006) and meteorological data measured at T1 to classify the wind direction prevailing from Mexico City, hence we classified the days with and without a clear influence of pollutants to sample particles with the impactors. Doran et al. (2007) have calculated forward and back trajectories of air masses at 1000 m above ground level over site T1 during daylight hours (06:00–18:00 LST), for a 20-day period during the month of March 2006. The most favorable conditions for transport from site T0 to site T1 were seen to occur on days 69, 70, 77, 78, 79, 81, 83, 86 and 87 (10–11, 18–20, 22, 24, 27–28 March). On days 71–76 (12–17 March) and day 82 (23 March) the back trajectories indicated that transport would have likely been from site T1 towards Mexico City and site T0.

## 2.2 TEM microscopy and elemental analysis of atmospheric particles

The morphology and elemental composition of atmospheric particles were obtained using a Transmission Electronic Microscope (TEM, CM 200 Phillips TEM-EDAX system). Energy Dispersive X-Ray Spectrometry (EDS, model CM-200 Phillips 147-5 with a Si (Li) detector of  $30 \text{ mm}^2$  active area) was used to determinate the elemental analysis of aggregates. EDS is coupled to TEM with a micro analyzer. EDS-spectra were acquired for 20 seconds of clock time, relative dead time minor 30 %, and 1000–1500 photon count at an accelerating voltage 200 kV using magnifications of 10 000–100 000 x. Ninety-nine EDS-spectra were obtained for both particle sizes during the campaign that corresponds to three particles analysis for each sample. The elemental analysis is semi-quantitative, so the elemental carbon reported is limited by the film coating of the grid (Laskin et al., 2005), which affects its accuracy.

Images were analyzed and border-based fractal dimensions were calculated for at least 30 individual particles per sample, based on their perimeter (Kindratenko et al., 1994). Fractal parameters for 500 particles were calculated. Samples were taken every other day from 1 to 15 March 2006 (at T1). With border-based fractal dimensions sorted by sizes and sampling times, the morphology and aerosol differences were studied. Dye et al. (2000) and Kindratenko et al. (1994) have observed aerosol morphology changes with  $D_f$ .

## 2.3 Border-based fractal dimension calculation

Particle digital images were processed using Scion Image software (<http://www.scioncorp.com/>) for image optimization and extraction of (x, y) particle coordinates analysis. The program additionally provides the particle's area and perimeter length in pixels. The particle border-based (perimeter) fractal dimension is then calculated by a FORTRAN code developed at the University of Connecticut (Newman, 2001; Mamani-Paco, 2004). The code used the definition of border-based fractal dimension obtained with the following equation (Kaye, 1994; Mandelbrot, 1967):

$$L(\lambda) = k\lambda^{1-D_f}$$

where  $L$  is the particle perimeter,  $\lambda$  is the particle's boundary step size (the length by which the perimeter is cut in smaller pieces),  $k$  is a positive constant factor, and  $D_f$  is the fractal dimension. A Richardson plot was used to obtain the slope and the corresponding fractal dimensions (Kaye, 1994).

## 3 Results

### 3.1 Meteorological conditions

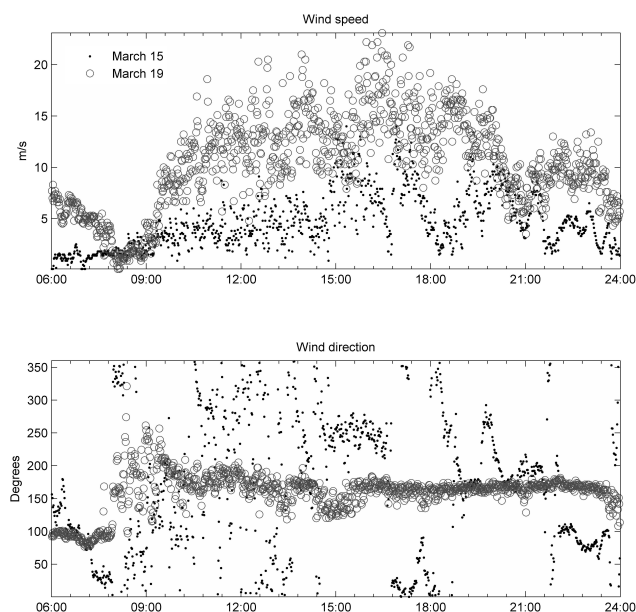
The meso-meteorological model, version 5, MM5 (de Foy et al., 2006) and the meteorological data recorded at T1 supersite provided information about the days with and without a clear MC plume influence. We chose Wednesday, 15 March 2006, and Sunday, 19 March 2006, to compare results, because they are clear days with different meteorological conditions that hamper or promote the pollutants transport emitted at MC to the site (Fast et al., 2007). On 15 March, wind direction changes very often prevailing northerlies, while on 19 March the wind prevails southerly, where MC is located. It was assumed that southerly winds carried pollutants from the urban area to the site. Also, samples obtained on those days were good for comparison. Figure 1 shows wind direction and speed time series (local time) for both days.

### 3.2 Optical properties of particles

Figure 2 shows time series for particle concentration, scattering coefficient ( $\sigma_{\text{sct}}$ ), absorption coefficient ( $\sigma_{\text{abs}}$ ), and single scattering albedo (SSA) on both days. On Wednesday, 15 March, early in the morning ( $\sim 07:00$ ) local sources generated 50 000 particles per cubic centimeter, within  $0.01 - 3 \mu\text{m}$  diameter, and around 10:00 the concentration decreased to 10,000. There were also episodes from 19:00 to 24:00 when the concentrations increased and gradually arrived to 40 000 particles per cubic centimeter. Temporary changes in meteorological conditions could cause a major accumulation of particles from 06:00 to 09:00 and from 21:00 to 24:00. Northerlies cold winds (Fig. 1) at T1 decreased temperatures, promoting a suitable condition to reduce the mixed layer height. On Sunday, 19 March, particles concentration

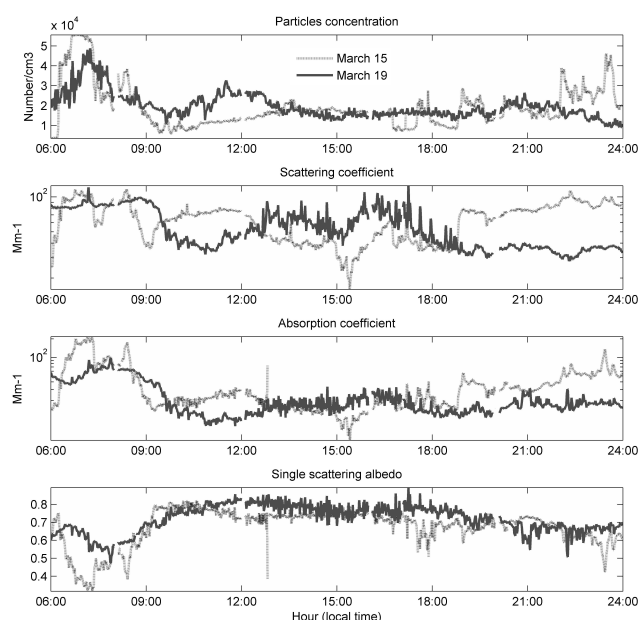
**Table 1.** Single scattering albedo (SSA) from three different sites.

Reference	Mexico City (T0)	Tecámac (T1)	Biznaga (T2)	Pico de Orizaba
Marley et al. (2009)	0.74	0.70		
Doran et al. (2007)			0.91	
Márquez et al. (2005)				0.92

**Fig. 1.** Time series for wind speed and direction at T1 on 15 and 19 March.

increased gradually from 09:00 to 13:00, when the plume of pollutants from MC arrived to T1. The little increase in particles number concentration on that day may also result from diluted plumes arriving earlier from MC (de Foy et al., 2006). Particles concentration decreased around 22:00, when the pollution activities ceased at Mexico City.

The scattering coefficient on 15 March increased again early in the morning and after 19:00, but decreased during 12:00 to 18:00. However, on 19 March the  $\sigma_{\text{scat}}$  fell down to  $40 \text{ Mm}^{-1}$  at 10:00, when the particles concentration increased. After 13:00, the scattering increased and finally at 19:00 the values remained at  $30 \text{ Mm}^{-1}$ . Perhaps, the high scattering values from 13:00 to 18:00 are caused by the presence of mixed and aged aerosols. That day was characterized by the influence of MC pollutants plume prevailing southerly winds (Fig. 1). At 21:00, both scattering and absorption coefficients decreased because pollution activities were less intensive. Also, the  $\sigma_{\text{scat}}$  values suggest that particles might have a complex chemical composition increasing light scattering. Baumgardner et al. (2007) concluded that sulfate-coated soot and other volatiles compounds favor scattering of radiation rather than absorption.

**Fig. 2.** Time series for particle concentration, absorption and scattering coefficients, and single scattering albedo for 15 and 19 March.

Episodes with high absorption coefficient values occurred along the mornings (06:00–09:00) on both days. Perhaps, they are caused by fresh vehicular emissions. However, 15 March values are higher than those from 19 March.  $\sigma_{\text{abs}}$  measured on 15 March may indicate an influence of local sources. On 19 March,  $\sigma_{\text{abs}}$  does not change much, from 12:00 to 24:00, matching with the southerly wind.

Figure 2 also shows the single-scattering albedo (SSA) calculated on both days. From 09:00 to 18:00, SSA values were ranged between 0.74–0.81. 15 March was affected by northerly winds (from Gulf of Mexico) and that day had a relative clean atmospheric background. Between 06:00 and 09:00, SSA lower values ( $\sim 0.3$ ) are probably caused by local fresh emissions. The minima values may be attributed to the presence of atmospheric particles with high  $\sigma_{\text{abs}}$ . Doran et al. (2007) reported similar values measured at T1, using a multi filter rotating shadow band radiometer.

Table 1 shows the total average for SSA values obtained at T1, compared against total averages from other measurements done in T0 (Mexico City), T2 (Rancho la Biznaga) during the MILAGRO campaign, and a rural area at Pico de

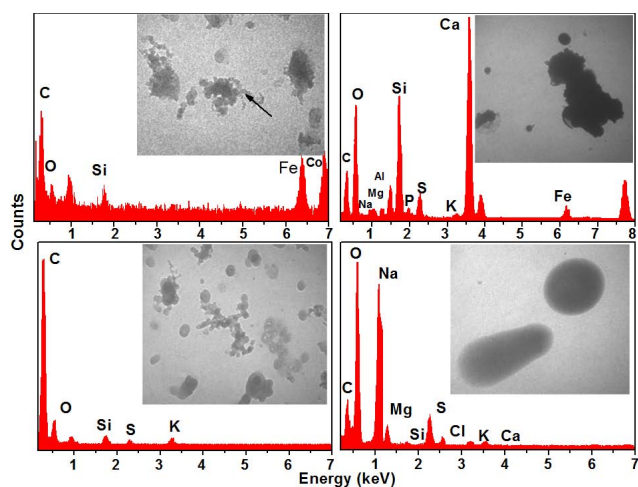


**Fig. 3.** TEM images and elemental analysis of atmospheric particles. Particles sampled on 15 March (row above) and 19 March (row below). Aerodynamic diameter  $0.18\ \mu\text{m}$  (left column) and  $1.8\ \mu\text{m}$  (right column).

Orizaba in 2004. Our study and Marley et al. (2009) share the same optical properties database. The SSA values obtained at T0 and T1 are smaller than those reported at T2 and Pico de Orizaba. In general behaviors, at T0 and T1 particles are probably a combination of local and nearby emissions. The SSA may change due to meteorology and human activities. T2 and Pico de Orizaba have both similar SSA (0.91 and 0.92, respectively), it seems that they have little local activities and they are far away from industrial or any other particle sources.

### 3.3 Particle morphology

Once meteorological conditions and particle optical characteristics were analyzed for 15 and 19 March, the morphology (border-based fractal dimension,  $D_f$ ) of small ( $d_{50} = 0.18\ \mu\text{m}$ ) and relatively larger ( $d_{50} = 1.8\ \mu\text{m}$ ) fine particles was determined to be used as an additional tool to distinguish local emitted and transported fine particles. Figure 3 shows particles TEM images for different sizes sampled at T1. Irregular shape particles were more common in smaller than in large sizes. Figure 4 shows small particles ( $d_{50} = 0.18\ \mu\text{m}$ ) collected at different sampling times; the arrow points to their main structure, which, in most cases, is composed of tiny spherules forming aggregates. This is a typical structure present in carbonaceous material originated in combustion processes. Irregular particle morphology can be noticed and soot chains are embedded in a complex matrix.

$D_f$  values are shown for specific morphologies. Figure 5 presents  $D_f$  histograms for small size particles ( $d_{50} = 0.18\ \mu\text{m}$ ) at different sampling times on both 15 and 19 March. Table 2 presents the basic statistics for this particle

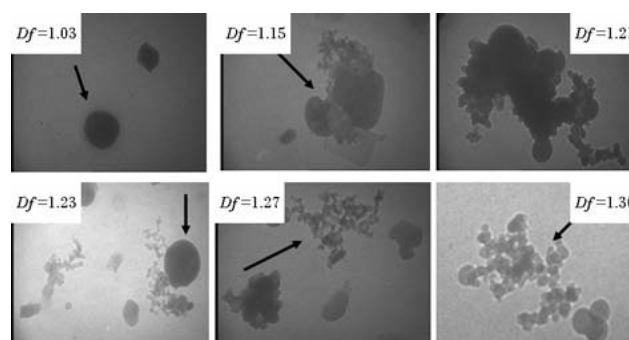


**Fig. 4.** TEM images with different border-based fractal dimension ( $D_f$ ) values for atmospheric particles with  $0.18\ \mu\text{m}$  aerodynamic diameter.

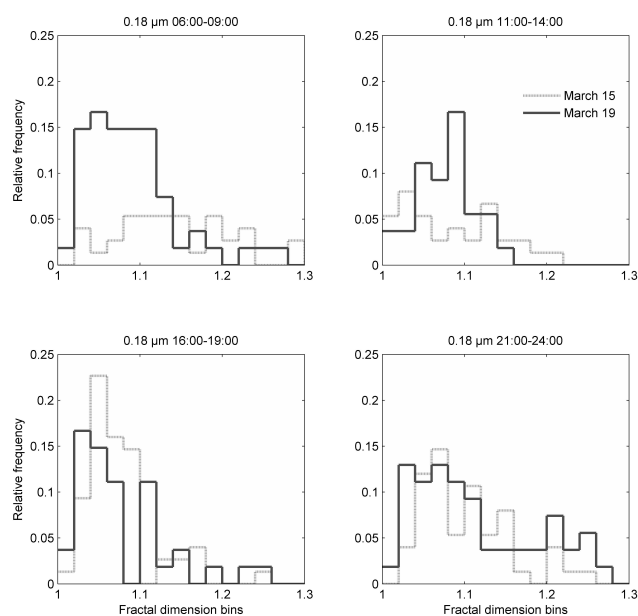


**Fig. 5.**  $D_f$  particles histograms ( $0.18\ \mu\text{m}$  aerodynamic diameter), sorted by sampling time. Relative frequency is defined as frequency of the observations in the  $D_f$  interval (Table 2).

size. Average  $D_f$  for particles sampled on 15 March between 06:00 and 09:00 was  $1.15 \pm 0.08$ , while average  $D_f$  for particles sampled on 19 March, at the same time, was  $1.10 \pm 0.06$ . The results for average  $D_f$  for the corresponding dates and sampling times (11:00–14:00) were  $1.09 \pm 0.06$  and  $1.08 \pm 0.06$ , respectively. There is a clear difference on frequency histograms between 15 and 19 March for the 06:00–09:00 sampling periods. It could be explained by the presence of freshly emitted aerosols on 15 March, and transported rounded aerosols on 19 March. Soot and metal aggregates can be emitted from local sources such as vehicle emissions and smelters. On 15 March, early in the morning (07:00), local sources generated 50 000 particles per cubic centimeter within  $0.01\text{--}3\ \mu\text{m}$  diameter, and around 10:00 the

**Table 2.** Fractal dimension statistics for atmospheric particles analyzed on TEM.

	Aerodynamic diameter = 0.18 $\mu\text{m}$							
	15 March				19 March			
	06:00	11:00	16:00	21:00	06:00	11:00	16:00	21:00
Number ( $N$ )	36	32	56	51	54	44	37	50
Minimum	1.03	1.01	1.01	1.03	1.01	1.02	1.01	1.02
Maximum	1.31	1.21	1.25	1.25	1.31	1.26	1.25	1.27
Average	1.15	1.09	1.07	1.09	1.10	1.08	1.08	1.11
Standard dev	0.08	0.06	0.04	0.05	0.06	0.06	0.06	0.07
Error ( $N$ ) <sup>1/2</sup>	0.15	0.12	0.13	0.18	0.16	0.18	0.15	0.17

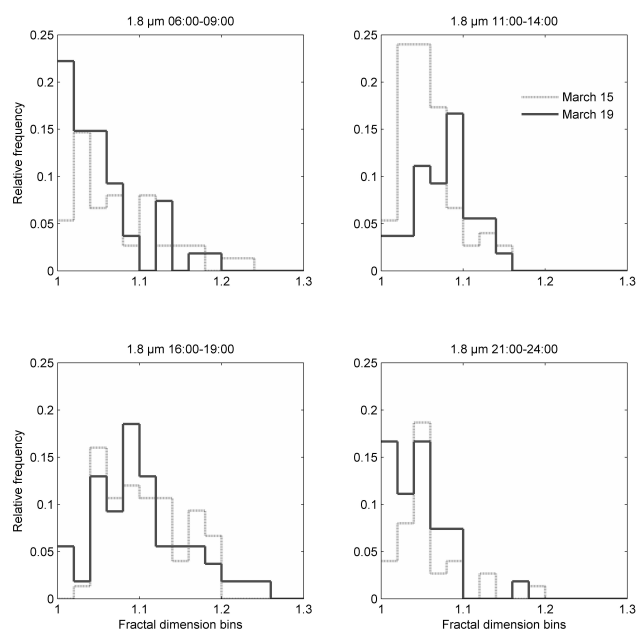
**Table 3.** Fractal dimension statistics for atmospheric particles analyzed on TEM.

	Aerodynamic diameter = 1.8 $\mu\text{m}$							
	15 March				19 March			
	06:00	11:00	16:00	21:00	06:00	11:00	16:00	21:00
Number ( $N$ )	42	65	61	31	41	32	47	33
Minimum	1.01	1.01	1.03	1.00	1.00	1.01	1.01	1.00
Maximum	1.23	1.16	1.19	1.18	1.20	1.32	1.24	1.18
Average	1.08	1.06	1.10	1.05	1.05	1.08	1.10	1.05
Standard dev	0.06	0.03	0.05	0.04	0.05	0.05	0.06	0.04
Error ( $N$ ) <sup>1/2</sup>	0.17	0.18	0.13	0.14	0.14	0.15	0.16	0.14

concentration decreased to 10 000 (Fig. 2). In Fig. 5 histograms for 16:00–19:00 and 21:00–24:00 sampling periods have similar distribution patterns in both days. In 16:00–19:00 sampling time, particles tend to be more spherical indicating that they are probably transported from Mexico City to T1. In 21:00–24:00, both distributions broadened to include more irregular shapes (higher border-based fractal dimension values). This is likely due to the presence of particles emitted from local sources.

The morphology of larger size fine particles ( $d_{50} = 1.8 \mu\text{m}$ ) is reported in Fig. 6 at different sampling times for both days, it was expected to be less irregular, tending to spherical, due to their typical sources (mechanical and chemical processes, aging, and combustion). Therefore, the border-based fractal dimension ( $D_f$ ) would tend to 1. The average  $D_f$  reported in Table 3 ranged from 1.10 to 1.05. These results agree with what was expected for particles in this size range. The histograms in Fig. 6, for 16:00–19:00 and 21:00–24:00 for both days, have similar patterns that cannot be distinguished one from another. But the histograms show a more uniform distribution of fractal dimensions in the period 16:00 to 19:00, and round shapes ( $D_f$  tends to 1) in the period 21:00–24:00, probably due to atmospheric physical and chemical processes on particles (i.e., aging).

In our study, it can be noted that particles with larger sizes tend to have a more spherical shape ( $D_f$  tends to 1.0). Particles with smaller sizes reflect the formation of soot with an

**Fig. 6.**  $D_f$  particles histograms (1.8  $\mu\text{m}$  aerodynamic diameter), sorted by sampling time. Relative frequency is defined as frequency of the observations in the  $D_f$  interval (Table 3).

**Table 4.** Elemental composition of atmospheric particles (1.8 and 0.18  $\mu\text{m}$  aerodynamic diameters) sampled on 15 and 19 March. Average results for particles analyzed in Fig. 3, weight percent.

Element	15 March		19 March	
	1.8 $\mu\text{m}$	0.18 $\mu\text{m}$	1.8 $\mu\text{m}$	0.18 $\mu\text{m}$
C	5.8	21.7	3.9	77.9
O	15.7	4.6	18.4	11.1
Na	4.7		67.7	
Mg	2.2		3.5	
Al	5.3			
Si	19	6.1	0.3	9
P	0.9			
S	3.9		4.0	
K	1		0.6	1.1
Ca	38		0.6	
Fe	3.4	33.3		
Co		34.3		

irregular characteristic fractal shape ( $D_f$  tends to 1.2–1.3) (Kindratenko et al., 1994; Mamani-Paco, 2004). This may indicate different steps in aerosol aging processes; i.e. soot particles are released to the atmosphere as agglomerates with voids, and as they age – by photochemical or condensation processes – they change their shape to spherical coated soot.

Particle concentration on 19 March increased gradually when the plume of pollutants from MC arrived to T1 (09:00 to 13:00), and decreased when the pollution activities ceased at Mexico City (around 22:00).

On 15 March, between 06:00 and 09:00 (Fig. 5), the frequency histogram indicates a high number of particles with irregular shapes that might be associated with fresh soot emissions (Dye et al., 2000), absorbing radiation efficiently and responsible for the absorption peak that appears early morning on that day (Fig. 2). Particle absorption coefficient values for 15 March are higher than those for 19 March, and those from 15 March point to an influence of local sources with smaller fine particles having highly irregular morphologies ( $D_f = 1.2\text{--}1.3$ ).

### 3.4 Elemental composition of particles

Twelve elements were detected on the samples analyzed by EDS. Table 4 presents averaged results from 36 analyses on relative elemental composition.

Elemental analyses performed on some particles (Fig. 3) show aggregates with internal mixing. It is evident that small aerodynamic diameter ( $d_{50} = 0.18\ \mu\text{m}$ ) has the highest percentage of C, Fe and Co in its structure. The last two elements could be released by local sources, such as oxidation in mechanical parts of cars, or metallurgical activities carried out near the area. In Mexico City fresh particulate emissions due to motor vehicle traffic, especially diesel engines, are mostly carbonaceous with very low sulfur content (Molina

and Molina, 2002), as it is illustrated on Table 4. Figure 3 shows particles observed in TEM with several crusted elements, like S, O, Si, Al, Ca, Ti, Mn, Fe, and K.

Particles with  $d_{50} = 1.8\ \mu\text{m}$  have low oxygen and carbon percentages, but high potassium levels (a biomass burning tracer), and other elements such as Si, Na, Ca, and Al; which are more abundant in clayey soils and rocks (Seinfeld and Pandis, 1998).

## 4 Conclusions

A previous study by Johnson et al. (2005) concluded that MC soot particles collected directly from city traffic were mostly irregular, and showed physical and chemical differences against soot particles collected in ambient conditions. Adachi and Buseck (2008), and Moffet et al. (2010) suggested a rapid aging process (in the order of hours) to spherical coated soot particles or embedded in an organic matrix in MC. We can then infer that irregular freshly emitted soot aggregates with high border-based fractal dimensions ( $D_f$  close to 2) become spherical coated soot particles ( $D_f$  close to 1) as a result of condensation and coagulation processes (aging). Mofet and Prather (2009) reached the same conclusion by studying soot particles in MC and Riverside. Our results for morphology differences between sampling times with and without MC plume influence at T1 site agree with those findings. It is important to note that images and morphological information described in this article only correspond to non-volatile components of particulate matter. Our work provides some initial quantification of changes in morphology at a specific particle size ( $d_{50} = 0.18\ \mu\text{m}$ ). Ramsden and Shibaoka (1982); Pósfai et al. (2003); Kaegi and Holzer (2003); Li et al. (2003); Dye et al. (2000) used a similar analysis approach to study aerosol particles properties. Information obtained with the quantification of ambient soot particle morphology may improve climate and health models.

Elemental composition analyses show different inclusions of inorganic grouped elements (S, K, and Si; Fe, Na, and P), which agree with earlier studies in Mexico City (Johnson et al., 2005). Sulfate inclusions and other components in transported soot particles are probably due to coagulation and collision processes experienced by aerosols in the atmosphere, which strongly affect their optical properties (Johnson et al., 2005; Marley et al., 2009; García et al., 2010).

Adachi and Buseck (2008) sampled particles on a C130 airplane during MILAGRO campaign and classified them, based on their sampling location (inside or outside MC plume of pollutants); they also used EDS to determine their elemental composition. They found very often S and K in particles ranged between 50–2000 nm size, and classified the structures as soot and organic matter. Our analysis shows that S and K contents in  $d_{50} = 0.18\ \mu\text{m}$  particles represent respectively around 3.9% and 1%; but it is difficult to compare results between both studies, specially because the C130

samples were taken around 3.1 km above T1, and represent freshly emitted particles, while our sampling was at the surface characterizing local and transported particles.

Moffet et al. (2010) analyzed particles sampled at T1 with different X-ray analytical techniques (i.e. microscopy and absorption), finding at T1 particles homogeneous with spherical shapes and mixed with organic compounds, in our study  $D_f$  tends to 1, indicating more spherical shapes. They also found high contents of Al, S, Ca, and Fe in particles sampled at T1, and stated that some element concentrations are due to local emissions. However, the morphology and elemental composition for both sizes (around 0.18 and 1.8  $\mu\text{m}$ ) are not conclusive to relate the particles origin with specific human activities in areas nearby T1.

**Supplement related to this article is available online at:**  
<http://www.atmos-chem-phys.net/12/2747/2012/acp-12-2747-2012-supplement.zip>.

*Acknowledgements.* The authors would like to thank M. I. Saavedra for helping them in the aerosols optical properties and gravimetric analyses. They want also thank L. Molina, J. Gaffney and S. Madronich for the facilities offered during MILAGRO campaign at T1. Also, to thank Dulce Nazareth Ramírez for her support on the document edition. Referees from ACP also give substantial ideas to enhance the quality of this study.

Edited by: A. Baklanov

## References

- Adachi, K. and Buseck, P. R.: Internally mixed soot, sulfates, and organic matter in aerosol particles from Mexico City. *Atmos. Chem. Phys.*, 8, 6469–6481, doi:10.5194/acp-8-6469-2008, 2008.
- Baumgardner, D., Raga, G. B., Kok, G. L., Ogren, J., Rosas, I., Baez, A., and Novakov, T.: On the evolution of aerosol properties at a mountain site above Mexico City, *J. Geophys. Res.*, 105, 17, 22243–22253, 2000.
- Baumgardner, D., Kok, G. L., and Raga, G. B.: On the diurnal variability of particle properties related to light absorbing carbon in Mexico City. *Atmos. Chem. Phys.*, 7, 2517–2526, doi:10.5194/acp-7-2517-2007, 2007.
- Bond, T. and Bergstrom, R.: Light absorption by carbonaceous particles: an investigative review, *Aerosol Sci. Technol.*, 39, 1–41, doi:10.1080/02786820500421521, 2005.
- De Foy, B., Varela, J. R., Molina, L. T., and Molina, M. J.: Rapid ventilation of the Mexico City basin and regional fate of the urban plume. *Atmos. Chem. Phys.*, 6, 2321–2335, doi:10.5194/acp-6-2321-2006, 2006.
- Doran, J. C., Barnard, J. C., Arnott, W. P., Cary, R., Coulter, R., Fast, J. D., Kassianov, E. I., Kleinman, L., Laulainen, N. S., Matin, T., Paredes-Miranda, G., Pekour, M. S., Shaw, W. J., Smith, D. F., Springston, S. R., and Yu, X. Y.: The T1-T2 study: evolution of aerosol properties downwind of Mexico City, *Atmos. Chem. Phys.*, 7, 1585–1598, doi:10.5194/acp-7-1585-2007, 2007.
- Dye, A. L., Rhead, M. M., and Trier, C. J.: The quantitative morphology of roadside and background urban aerosol in Plymouth, UK, *Atmos. Environ.*, 34, 3139–3148, 2000.
- Fast, J. D., de Foy, B., Acevedo Rosas F., Caetano E., Carmichael, G., Emmons, L., McKenna, D., Mena, M., Skamarock, W., Tie, X., Coulter, R. L., Barnard, J. C., Wiedinmyer, C., and Madronich, S.: A meteorological overview of the MILAGRO field campaigns. *Atmos. Chem. Phys.*, 7, 2233–2257, 2007, <http://www.atmos-chem-phys.net/7/2233/2007/>.
- García, L. Q., Castro, T., Saavedra, M. I., and Martínez-Arroyo, M. A.: Optical properties of aerosols: southern Mexico City, *Atmósfera*, 23, 403–408, 2010.
- Horvath, H., Catalan, L., and Trier, A.: A study of the aerosol of Santiago de Chile III Light absorbing measurements, *Atmos. Environ.*, 31, 3737–3744, 1997.
- Jiménez, J. C., Raga, G. B., Baumgardner, D., Castro, T., Rosas, I., and Báez, A.: On the composition of aerosol particles influenced by emissions of the volcano Popocatepetl in Mexico, *Natural Haz.*, 31, 21–37, 2004.
- Johnson, K. S., Zuberi, B., Molina, L. T., Molina, M. J., Iedema, M. J., Cowin, J. P., Gaspar, D. J., Wang, C., and Laskin, A.: Processing of soot in an urban environment: Case study from the Mexico City Metropolitan Area, *Atmos. Chem. Phys.*, 5, 3033–3043, doi:10.5194/acp-5-3033-2005, 2005.
- Kaegi, R. and Holzer, L.: Transfer of a single particle for combined ESEM and TEM analyses, *Atmos. Environ.*, 37, 4353–4359, 2003.
- Katrinak, K. A., Rez, P., Perkess, P. R., and Buseck, P. R.: Fractal geometry of carbonaceous aggregates from an urban aerosol, *Environ. Sci. Technol.*, 27, 539–547, 1993.
- Kaye, B. H.: *A Random Walk through Fractal Dimensions*, 427 pp., 2nd edition, Weinheim; Base 1 (Switzerland); Cambridge; New York, NY, VCH, 1994.
- Kindratenko, V. V., Van Espen, J. M., Treiger, B. A., Van Grieken, R. E.: Fractal dimensional classification of aerosol particles and computer-controlled scanning electron microscopy. *Environ. Sci. Technol.*, 28:2197-2202, 1994.
- Laskin, A., Cowin, J. P., and Iedema M. J.: Analysis of individual environmental particles using modern methods of electron microscopy and X-ray microanalysis, *J. Electr. Spectrosc. Rel. Phenom.*, 150, 260–274, 2005.
- Li, J., Anderson, J. R., and Buseck, P. R.: TEM study of aerosol particles from clean and polluted marine boundary layers over the North Atlantic, *J. Geophys. Res.*, 108, 4189, doi:10.1029/2002JD002106, 2003.
- Li, W. and Shao, L.: Transmission electron microscopy study of aerosol particles from the brown hazes in northern China. *J. Geophys. Res.*, 114, D09302, doi:10.1029/2008JD011285, 2009.
- Mandelbrot, B. B.: How long is the coastline of Britain? Statistical self similarity and fractional dimension, *Science*, 156, 636–638, 1967.
- Mamani-Paco, R.: Morphology distributions and chemical composition of size-selected atmospheric fine particles. PhD dissertation, AAT 3156402, ISBN 0496171003, University of Connecticut, Storrs, CT, USA, 2004.
- Mamani-Paco, R. M. and Heble, J. J.: Particle size and time of the day influences on the morphology distributions of atmospheric fine particles at the Baltimore supersite, *Atmos. Environ.*, 41, 8021–8029, 2007.

- Marley, N. A., Gaffney, J. S., Castro, T., Salcido, A., and Frederick, J.: Measurements of aerosol absorption and scattering in the Mexico City Metropolitan Area during the MILAGRO field campaign: a comparison of results from the T0 and T1 sites. *Atmos. Chem. Phys.*, 9, 189–206, doi:10.5194/acp-9-189-2009, 2009.
- Márquez, C., Castro, T., Muhlia, A., Martínez-Arroyo, M. A., and Báez, A.: Measurement of aerosol particles, gases and flux radiation in the National Park Pico de Orizaba, and its relationship to air pollution transport. *Atmos. Environ.*, 39, 3877–3890, 2005.
- Moffet R. C. and Prather, K. A.: In-situ measurements of the mixing state and optical properties of ssot with implications for radiative forcing estimates, *PNAS*, 106, doi:10.1073/pnas.0900040106, 2009.
- Moffet, R. C., Henn, T. R., Tivanski, A. V., Hopkins, R. J., Desyaterik, Y., Kilcoyne, A. L., Tyliczszak, D. T., Fast, J., Barnard, J., Shutthanandan, V., Cliff, S. S., Perry, K. D., Laskin, A., and Gilles, M. K.: Microscopic characterization of carbonaceous aerosol particle aging in the outflow from Mexico City, *Atmos. Chem. Phys.*, 10, 961–976, doi:10.5194/acp-10-961-2010, 2010.
- Molina, L. T. and Molina, M. J.: *Air quality in the Mexico Megacity, An integrated assessment*, Kluwer Academic, The Netherlands, 408 pp., 2002.
- Molina, L. T., Madronich, S., Gaffney, J. S., Apel, E., de Foy, B., Fast, J., Ferrare, R., Herndon, S., Jiménez, J. L., Lamb, B., Osornio-Vargas, A. R., Russell, P., Schauer, J. J., Stevens, P. S., Volkamer, R., and Zavala, M.: An overview of the MILAGRO 2006 Campaign: Mexico City emissions and their transport and transformation, *Atmos. Chem. Phys.*, 10, 8697–8760, doi:10.5194/acp-10-8697-2010, 2010.
- Mogo, S., Cachorro, V. E., and De Frutos, A. M.: Morphological, chemical and optical absorbing characterization of aerosols in the urban atmosphere of Valladolid, *Atmos. Chem. Phys.*, 5, 2739–2748, doi:10.5194/acp-5-2739-2005, 2005.
- Newman, M.: *Structural characterization of ambient particulate matter using fractal dimensions*, University of Connecticut, USA, CHEG 299, 2001.
- Okada, K. and Heintzenberg, J.: Size distribution, state of mixture, and morphology of urban aerosol particles at given electrical mobilities, *J. Aerosol Sci.*, 34, 1539–1553, 2003.
- Paredes-Miranda, G., Arnott, W. P., Jiménez, J. L., Aiken, A. C., Gaffney, J. S., and Marley, N. A.: Primary and secondary contributions to aerosol light scattering and absorption in Mexico City during the MILAGRO 2006 campaign, *Atmos. Chem. Phys.*, 9, 3721–3730, doi:10.5194/acp-9-3721-2009, 2009.
- Pope III, C. A. and Dockery D. W.: Health effects of Fine Particulate Air Pollution: Lines that connect, *J. Air Waste Manage. Assoc.*, 56, 709–742, 2006.
- Pósfai, M., Simonics, R., Li, J., Hobbs, P. V., and Buseck, P. R.: Individual aerosol particles from biomass burning in southern Africa: 1. Composition and distributions of carbonaceous particles. *J. Geophys. Res.*, 108, 8483, doi:10.1029/2002JD002291, 2003.
- Raga, G., Baumgardner, D., Castro, T., Martínez-Arroyo, M. A., and Navarro-González, R.: Mexico City Air Quality: A Qualitative Review of Gas and Aerosol Measurements (1960–2000). *Atmos. Environ.*, 35, 4041–4058, 2001.
- Ramsden, A. R. and Shibaoka, M.: Characterization and analysis of individual fly-ash particles from coal-fired power stations by a combination of optical microscopy, electron microscopy and quantitative electron microprobe analysis, *Atmos. Environ.*, 16, 2191–2206, 1982.
- Salcedo, D., Onasch, T. B., Dzepina, K., Canagaratna, M. R., Zhang, Q., Huffman, J. A., De Carlo, P. F., Jayne, J. T., Mortimer, P. Worsnop, D. R., Kolb, C. E., Johnson, K. S., Zuberi, B., Marr, L. C., Volkamer, R., Molina, L. T., Molina, M. J., Cárdenas, B., Bernabé, R. M., Márquez, C., Gaffney, J. S., Marley, N. A., Laskin, A., Shutthanandan, V., Xie, Y., Brune, W., Leshner, R., Shirley, T., and Jiménez, J. L.: Characterization of ambient aerosols in Mexico City during the MCMA-2003 campaign with aerosol mass spectrometry: results from the CENICA Supersite. *Atmos. Chem. Phys.*, 6, 925–946, doi:10.5194/acp-6-925-2006, 2006.
- Seinfeld, J. H. and Pandis, S. N.: *Atmospheric chemistry and physics: from air pollution to climate change*, A Wiley-Interscience publication, USA, 1326 pp., 1998.
- Tsuji, J. S., Maynard, A. D., Howard, P. C., James, J. T., Lam, C., Warheit, D. B., Santamaria, A. B.: Research strategies for safety evaluation of nanomaterials, part IV: risk assessment of nanoparticles, *Toxicol. Sci.*, 89, 1, 42–50, 2006.
- Xiong, C. and Friedlander, S. K.: Morphological properties of atmospheric aerosol aggregates, *PNAS*, 98, 11851–11856, doi:10.1073/pnas.211376098, 2001.